

<https://doi.org/10.1038/s42004-025-01680-2>

High-throughput glycosylation screening method for biologics development using MALDI-TOF-MS

Weilong Zhang¹, Liqi Xie², Huijuan Zhao¹, Xiaonan Ma¹ & Shifang Ren¹

Glycosylation is a critical quality attribute of therapeutic proteins, yet current analytical methods often fail to meet rapid, high-throughput demands. Here, we adopted an optimized glycosylation analysis method for the quality control of therapeutic proteins that combines the speed of MALDI-TOF-MS with the precision of a full glycome internal-standard approach. With 96-well-plate compatibility, the method enables the analysis of at least 192 samples in a single experiment and offers a highly promising solution for biopharmaceutical quality-control scenarios that demand both speed and high throughput capabilities. The suitability of the method was validated on trastuzumab (Herceptin[®]) with high precision (CV ~ 10%) and broad linearity ($R^2 > 0.99$) as well as fusion proteins (EPO) with multiple glycosylation sites and complex glycan structures. Excellent linearity, repeatability, and stability were demonstrated in the qualification study. The method offers significant benefits for characterizing N-glycans in glycosylated biologics, with applications ranging from early clone selection to batch-to-batch consistency control, as well as comparative assessments between biosimilars and reference drugs.

More than two-thirds of protein-based biologics undergo glycosylation¹, with N-glycosylation playing a significant role in the efficacy, stability, and safety of glycoprotein therapeutics^{2–4}. These proteins include monoclonal antibodies (mAbs)^{5,6} and highly glycosylated fusion proteins, such as erythropoietin (EPO)¹. For example, the glycosylation pattern of monoclonal antibodies can directly affect drug efficacy, such as antibody-dependent cell-mediated cytotoxicity (ADCC) or complement-dependent cytotoxicity (CDC)^{5,7,8}, whereas in EPO, it influences bioactivity, pharmacokinetics, immunogenicity and solubility^{9,10}. As the biopharmaceutical market continues to expand, driven by patent expirations of first-generation mAbs and the growth of biosimilars, the demand for efficient and reliable glycosylation analysis methods has increased^{11,12}. This increasing need is further prompted by the development of innovative biologics, which require extensive quality control procedures to meet regulatory guidelines and ensure product efficacy.

Glycan analysis is critical at numerous key points throughout the development, production, and commercialization of biopharmaceuticals. At different stages, the demand for rapid and high throughput screening methods for glycosylation quality control becomes particularly urgent. For example, during cell line and clone selection, large-scale screening requires high throughput, quick and reliable glycan profiling to identify cell lines that produce proteins with the desired glycosylation patterns^{13,14}. Additionally, in

process development and optimization, rapid and high throughput glycan analysis is essential to ensure consistent glycosylation profiles across various production conditions, such as culture conditions and media composition^{15–17}. Furthermore, the comparison between biosimilars and originators demands precise yet rapid glycan analysis to confirm the similarity in critical quality attributes. Batch release and stability studies also benefit from rapid screening methods, enabling faster quality assurance and ensuring that glycosylation patterns remain consistent over time¹⁸.

MALDI-TOF-MS-based glycomics has emerged as a powerful tool for analyzing released free glycans from glycoproteins, offering exceptionally rapid analysis capable of processing hundreds of samples within minutes. However, its application in biologics quality control remains rare, primarily due to challenges in quantitative accuracy and reproducibility. To address these limitations, we adopted our previously established full glycome internal standard approach, which significantly improves quantification precision by matching each glycan with a corresponding glycan internal standard¹⁹. To meet the demands of rapid and high-throughput biopharmaceutical quality control applications, we applied an optimized glycosylation analysis method by replacing Cotton HILIC SPE with CL-4B Sepharose beads which have enhanced 96-well plate compatibility and analysis throughput. The method's effectiveness for quality control was demonstrated by analyzing glycans released from

¹NHC Key Laboratory of Glycoconjugates Research, Department of Biochemistry and Molecular Biology, School of Basic Medical Sciences, Fudan University, Shanghai, China. ²Shanghai Tanshi Biotechnology Co., Ltd., Pudong Shanghai, Shanghai, China. ✉e-mail: renshifang@fudan.edu.cn

the trastuzumab originator Herceptin® and applying it to more complex glycoprotein biologics.

In this study, we offer a robust solution for rapid and reliable glycosylation analysis in biopharmaceutical development and manufacturing. It represents novel attempt to apply the approach based on MALDI-TOF MS for biopharmaceutical quality control. This strategy not only significantly accelerates the screening process but also provides precise quantitative information on glycans. This method holds promise as a key tool in glycoprotein drug development, supporting the optimization of production processes, enhancing product consistency, and advancing technological innovation in the biopharmaceutical field.

Results

Development of the workflow

Previously, our group developed an N-glycomics analytical method that utilizes one step reaction of reductive isotope labeling to generate full glycome internal standards. By employing a one-step process of glycan reduction and isotope labeling, these glycans acquire a mass of 3 Da higher than their native counterparts. Once obtained, the internal standards are mixed with the samples under analysis, forming a broad-coverage N-glycan internal standard library. Because the library and native N-glycans share identical compositions and similar relative abundances, it enhances the accuracy of glycan quantification.

To adopt the method's applicability in high-throughput biologics quality control, we used the optimized method different from the original protocol. First, during the purification and enrichment steps, degreased cotton in the Cotton HILIC SPE was replaced with CL-4B Sepharose beads²⁰, creating the "Sepharose HILIC SPE." Second, the entire purification processes are transferred to 96-well plates, significantly improving both the

throughput and efficiency of internal standard preparation. These modifications also allow full automation on a liquid handling robotic workstation. Furthermore, we now vacuum-dry the internal N-glycans at room temperature and store them at -80°C , rather than storing small volumes in water. This revised procedure not only enhances sample stability and yields but also makes large-scale analyses more feasible. An overview of the rapid glycosylation screening method is presented in Fig. 1.

Qualification of the workflow

We determined the precision of the method by assessing the repeatability and intermediate precision of the entire process. Specificity was confirmed by overlaying mass spectrum, which revealed no corresponding peaks in the N-glycan region of the control, thereby demonstrating the absence of interfering variables. In the repeatability test, the coefficient of variation (CV) for six repeated analyses performed on a single day ranged from 6.44% to 12.73%, with an average of 10.41%. The intermediate precision over three days also remained stable, with CVs ranging from 8.93% to 12.83%, with an average of 10.78%. The linear range was evaluated using a 75-fold concentration gradient. All 192 samples were processed simultaneously from preparation to final data acquisition, with each sample measurement completed within seconds. Quantitative results can typically be obtained within an hour using automated data processing. In the following sections, we will discuss these aspects in detail, including specificity, repeatability, linear range, etc.

Specificity

To ensure the reliability of rapid quality control outcomes, avoiding the inclusion of any potential confounding variables during sample preparation is crucial. The trastuzumab originator Herceptin® buffer was used as a

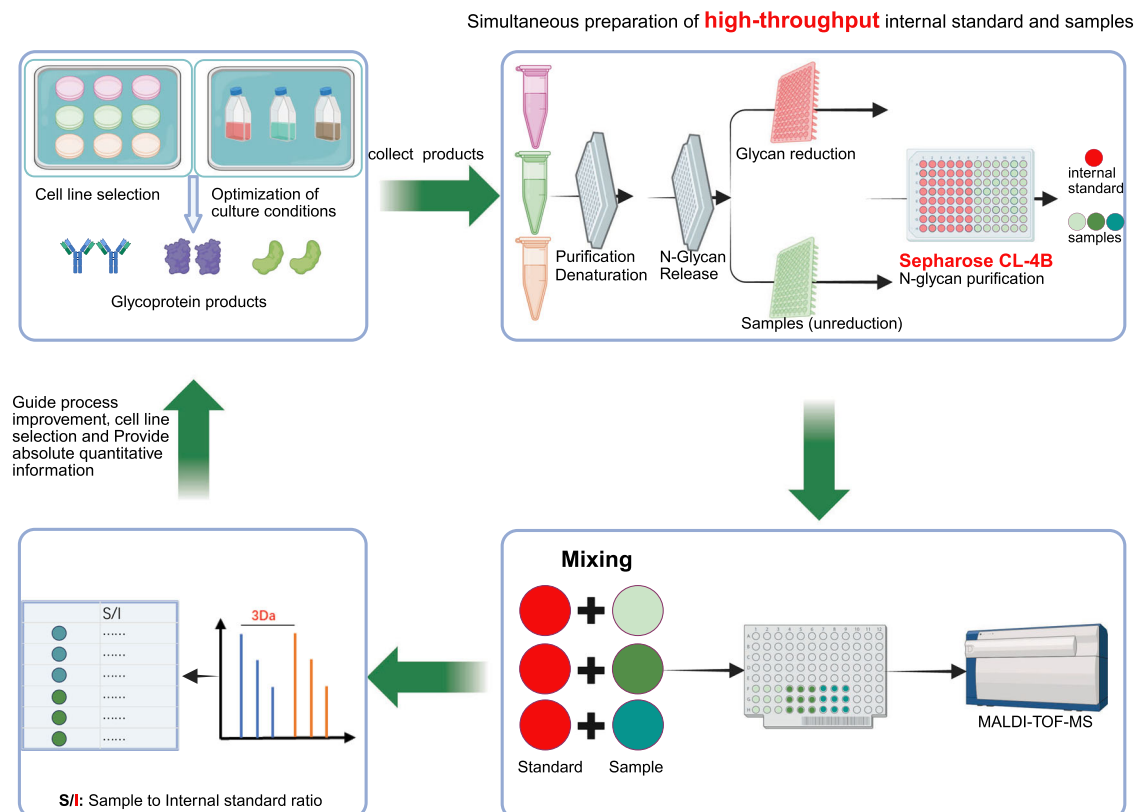


Fig. 1 | Schematic of the rapid glycosylation screening method. This method is suitable for the rapid characterization of N-glycosylation across multiple glycoprotein production steps (upper left section). By collecting the products and simultaneously preparing internal standards for high-throughput sample analysis (upper right section), coupled with the high-speed analysis capability of MALDI-

TOF-MS (lower right section), accurate glycan content information is obtained (lower left section). This enables the optimization of production conditions and guides the selection of production cell lines. The manual workflow processes up to 192 samples per run and is completed in ~8–9 h; a detailed timeline is provided in Supplementary Table1.

control and was prepared in parallel with the sample to maintain analytical consistency. By overlaying the mass spectrum of the buffer with those of the sample, we observed a complete absence of corresponding peaks in the N-glycan region, confirming that no peaks from the sample appeared in the buffer spectrum. Furthermore, the buffer spectrum exhibited minimal identifiable peaks, confirming that no extraneous substances capable of interfering with N-glycan identification were introduced throughout the procedure (Supplementary Fig. 1). These findings substantiate the high specificity of our rapid glycosylation screening strategy.

Repeatability and intermediate precision

To qualify the stability of the overall experimental workflow, we processed six replicate trastuzumab samples within a single day and measured three replicates on each of two additional days to assess repeatability and intermediate precision. The repeatability of all analytes, expressed as CV, ranged from 6.44% to 12.73%, with an average of 10.41%. Notably, even for glycans with a low abundance of 0.2% (G0FB), good repeatability (7.5%) was achieved. The analysis of 12 trastuzumab samples collected over three different days revealed CV ranging from 8.93% to 12.83%, with an average of 10.78% (Table 1). The results indicate that, despite full manual operation, the variability between the results obtained on different analysis days was minimal.

Linear range

A good linear range is essential for the accuracy of quantification. To rigorously evaluate the linear range of our method, we investigated the quantification performance across a 75-fold concentration range, which included the validation sample concentration. Our method was applied to analyze gradient dilutions of 1 \times , 1.5 \times , 2.25 \times , 3.375 \times , 5.0625 \times , and 7.59375 \times (actual concentrations scaled by a factor of 10). The results revealed R^2 values exceeding 0.9818, up to 0.9985, with an average of 0.9937 (Fig. 2a). These findings indicate that our method has excellent linearity over a wide concentration range, accurately reflecting the conditions of the samples.

Furthermore, because our method incorporates an internal standard glycan for each target glycan, it enables absolute quantification via an external standard glycan. We assessed the feasibility of quantifying the absolute amount of G2F in antibody drugs via the standard glycan G2F. When the standard curve was constructed with G2F combined with the full internal standard, the results showed excellent linearity for G2F within the concentration range of 0.78–6.25 nmol ($R^2 = 0.9989$) (Fig. 2b). This finding suggests that we can use the same internal standard to quantify the amount of G2F in samples.

Advantages of internal-standard quantification

All sample-preparation steps were performed in a 96-well format with Sepharose CL-4B HILIC plates in place of hand-packed cotton tips. The MALDI-TOF-MS spectra obtained with the Sepharose workflow were virtually indistinguishable from those generated with the cotton-tip protocol (Supplementary Fig. 2). Composition-level analysis revealed only subtle differences between the two media, seen chiefly for H4N4, H3N5F1, and H4N4F1E1 (Fig. 3a).

The benefit of the reduced internal standard was assessed with N-glycans released from human-serum IgG in two parallel workflows: one without internal standards, in which glycan abundances were expressed as the percentage of the total signal intensity; and one with internal standards, in which each glycan was quantified as the ratio of its signal intensity to that of its corresponding internal standard.

Subsequently, both sample sets were spiked with a known amount of the G0F glycan to simulate fluctuations in glycan abundance. Prior to spiking, we confirmed that the amount of G0F used fell within the linear response range of our internal standard-based quantification method (Fig. 3b).

When comparing the spiked results to the baseline (non-spiked) values, the internal standard approach correctly reflected a selective increase in G0F signal, while the levels of all other glycans remained essentially

unchanged (Fig. 3c). In contrast, in the absence of internal standards, the increase in G0F was also observed, but the apparent levels of all other glycans decreased (Fig. 3d), due to the constraint that relative abundances must sum to 100%.

These findings demonstrate that the internal standard method accurately attributes the change to G0F alone, whereas another method may suggest a global shift in the glycan profile.

Application in cell line selection

Four trastuzumab lots collected at the monoclonal cell selection stage were examined to evaluate the workflow under manufacturing conditions. UHPLC profiling identified six N-glycans—Man5, G0F-GN, G0, G0F, G1F and G0FB—present in all lots and spanning 0.1–80.5% relative abundance. These glycans (labelled Glycan1–6) were quantified by MALDI-TOF-MS using the +3 Da internal standard and compared with UHPLC values.

The MALDI data reproduced the up- and down-trends observed by UHPLC across the four lots (Fig. 4a and Supplementary Fig. 3); a single deviation was noted for glycan 4 in lot 4. Linear regression of the two datasets yielded a near-unity slope over the entire range (Fig. 4b and Supplementary Fig. 4). MALDI detected differences as small as 0.08%, as exemplified by G0F-GN, which was present at 0.20% in lot 1 and 0.12% in lot 3 (Fig. 4c, d). Prompted by these observations, we re-analyzed the same batch of samples by MALDI-MS both with (+IS) and without (–IS) internal standards. When glycan abundances exceeded 10%, the two workflows showed similarly good reproducibility (coefficients of variation, CVs: +IS = 5.53% and 3.32%; –IS = 2.48% and 2.79%; Fig. 4e). Below this threshold (< 10%), the +IS method continued to provide consistent precision (CVs: 12.77%, 2.58%, and 4.74%; Fig. 4f), whereas the –IS data exhibited broader scatter (CVs: 41.6%, 22.93%, and 21.84%; Fig. 4f). Consequently, at low abundances the larger variability observed in the –IS results can make real differences between samples more difficult to discern (Fig. 4g).

This subtle difference is particularly critical for biotherapeutics such as Herceptin[®], whose efficacy partly relies on antibody-dependent cellular cytotoxicity (ADCC). During manufacturing, afucosylated and high-mannose glycans must be tightly controlled; for example, the high-mannose fraction (%HM) should remain below 2%, while increases to $\geq 5\%$ can noticeably affect function²¹. Under such stringent requirements, the +IS MALDI-MS workflow provides the robustness required for confident quantitation of trace-level glycans, whereas the –IS approach, although suitable for higher-abundance species, may benefit from supplementary verification when very low-level glycans are of interest.

Given the limited throughput of UHPLC, the MALDI assay can perform the initial screen. If the acceptance window for glycan 1 is defined as $\pm 10\%$ of the value in lot 1 ($S/I = 0.3389; 0.305–0.373$), the MALDI read-out would retain lot 2 (0.3122) and exclude lots 3 (0.1932) and 4 (2.5500), reserving UHPLC for confirmatory analysis of the single candidate that meets the specification. This tiered strategy streamlines clone selection while preserving quantitative rigour.

Stability of sialic acid detection

During the qualification of four industrial samples, Sample 1 (S1) presented a relatively high level of sialylated glycan abundance. The two sialylated glycans present in S1 were identified as G1F + SA and G2F + SA, both of which are α 2,3-linked glycans. These two sialylated N-glycans were selected as target glycans to validate the stability of our rapid screening method for detecting sialic acid. After re-preparing the S1 sample and internal standard, we implemented a glycan derivatization step to protect the sialic acid prior to analysis. The experiment was repeated once per day for three consecutive days to validate the stability of our method following sialic acid addition. The results revealed that the three-day stabilities (expressed as CV values) of G1F + SA and G2F + SA were 9% and 13.2%, respectively. Moreover, nonsialylated glycans such as G0, G0F, and G1F had three-day CV values of approximately 10% (details presented in Table 2), indicating that adding a sialic acid protection step had a minimal impact on the overall rapid

Table 1 | Repeatability and intermediate precision

Glycan	Putative Structure	Composition	DAY1 (Mean ± SD)						Reproducibility CV	DAY2 (Mean ± SD)			DAY3 (Mean ± SD)			Cross Day CV
			1	2	3	4	5	6		1	2	3	1	2	3	
G0-GN		H3N3	0.320 ± 0.016	0.307 ± 0.006	0.328 ± 0.019	0.344 ± 0.007	0.273 ± 0.013	0.376 ± 0.010	10.76%	0.315 ± 0.018	0.352 ± 0.018	0.306 ± 0.031	0.340 ± 0.016	0.353 ± 0.004	0.383 ± 0.044	9.46%
Man5		H5N2	0.295 ± 0.005	0.281 ± 0.006	0.291 ± 0.008	0.295 ± 0.005	0.232 ± 0.003	0.348 ± 0.005	12.73%	0.255 ± 0.026	0.296 ± 0.013	0.238 ± 0.015	0.265 ± 0.006	0.280 ± 0.008	0.298 ± 0.033	11.08%
G0F-GN		H3N3F1	0.293 ± 0.008	0.252 ± 0.006	0.286 ± 0.010	0.291 ± 0.004	0.226 ± 0.004	0.314 ± 0.004	11.53%	0.227 ± 0.025	0.266 ± 0.013	0.214 ± 0.014	0.270 ± 0.003	0.285 ± 0.011	0.280 ± 0.030	11.61%
G0		H3N4	0.289 ± 0.008	0.278 ± 0.004	0.293 ± 0.010	0.294 ± 0.005	0.237 ± 0.006	0.344 ± 0.005	11.86%	0.261 ± 0.027	0.302 ± 0.021	0.246 ± 0.021	0.279 ± 0.008	0.294 ± 0.004	0.314 ± 0.035	10.18%
G0F		H3N4F1	0.587 ± 0.026	0.543 ± 0.024	0.552 ± 0.024	0.525 ± 0.034	0.485 ± 0.022	0.563 ± 0.022	6.44%	0.464 ± 0.035	0.483 ± 0.037	0.422 ± 0.030	0.470 ± 0.019	0.462 ± 0.020	0.439 ± 0.009	10.57%
G1F		H4N4F1	0.303 ± 0.005	0.269 ± 0.003	0.303 ± 0.011	0.311 ± 0.008	0.244 ± 0.006	0.341 ± 0.004	11.45%	0.248 ± 0.027	0.279 ± 0.017	0.233 ± 0.016	0.303 ± 0.001	0.313 ± 0.009	0.313 ± 0.034	11.55%
G0FB		H3N5F1	0.446 ± 0.013	0.428 ± 0.012	0.453 ± 0.014	0.496 ± 0.009	0.403 ± 0.004	0.479 ± 0.009	7.50%	0.438 ± 0.014	0.463 ± 0.062	0.442 ± 0.047	0.502 ± 0.017	0.542 ± 0.006	0.527 ± 0.036	8.93%
G2F		H5N4F1	0.303 ± 0.005	0.379 ± 0.016	0.416 ± 0.014	0.461 ± 0.033	0.350 ± 0.032	0.459 ± 0.043	11.02%	0.388 ± 0.036	0.428 ± 0.074	0.376 ± 0.062	0.477 ± 0.034	0.507 ± 0.011	0.517 ± 0.080	12.83%

glycosylation screening workflow (requiring only an additional 1.5 hours). Therefore, we conclude that our method is applicable for quantifying sialylated glycans and can also distinguish between α 2,3- and α 2,6-linked sialic acid isomers.

Application to other glycoprotein biopharmaceuticals

In addition to monitoring glycosylation during monoclonal antibody production, other glycoprotein biopharmaceuticals also require stringent glycosylation monitoring. Erythropoietin (EPO) is a highly glycosylated hormone that stimulates red blood cell production, with approximately 40% of its molecular mass composed of N-glycan or O-glycan conjugates^{9,22,23}. The sialic acid content and the antenna structure of glycans are two critical quality attributes that significantly impact EPO biological activity^{10,24}. We applied our rapid screening method for the detection of EPO N-glycans and achieved excellent results. Following previously reported workflows, the target N-glycans used for method validation included H6N2P1, H5N4F1S2, H6N5F1S2, H6N5F1S3, H7N6F1S2, H7N6F1S3, H7N6F1S4, and H8N7F1S3 (H = Hexose, N = N-acetylhexosamine, F = Fucose, S = N-acetylneuraminic acid, P = Phosphorylation of a high-mannose glycan) (Supplementary Fig. 5)²⁵. We prepared three identical samples over three consecutive days to validate the intermediate precision of our method for EPO detection. The results revealed that the three-day CV values for the eight N-glycans ranged from 2.05% to 12.75%, with an average of 8.45%,

indicating good stability (Table 3). In addition, owing to differences in the pretreatment process compared with trastuzumab, we also performed linearity validation of the EPO full glycan internal standard quantification method. The EPO N-glycan stock solution was serially diluted 0.33-fold to 7.5045-fold. The results revealed that all target glycans had R^2 values greater than 0.97, with most exceeding 0.99, demonstrating excellent linearity (Supplementary Fig. 6). These results indicate that our rapid glycan screening method is suitable for N-glycan detection in EPO, a complex glycoprotein preparation, suggesting its potential applicability for N-glycan detection in a broader range of glycoprotein biopharmaceuticals.

Discussion

This study demonstrated that our MALDI-MS-based glycan screening method is highly efficient for analyzing the N-glycan patterns of biologics. MALDI-TOF-MS provides considerable advantages for rapid screening of large sample volumes; however, reproducibility issues have historically posed challenges for accurate glycan identification²⁶. To address these issues, we developed a full-glycome internal standard that significantly enhances the quantitative accuracy of MALDI-TOF-MS. By adding the same internal standard to each sample, our method enables a rapid comparison of glycan content both within and between batches of monoclonal antibody batches, significantly reducing workflow time. Isolating the released glycans allows for accurate detection of

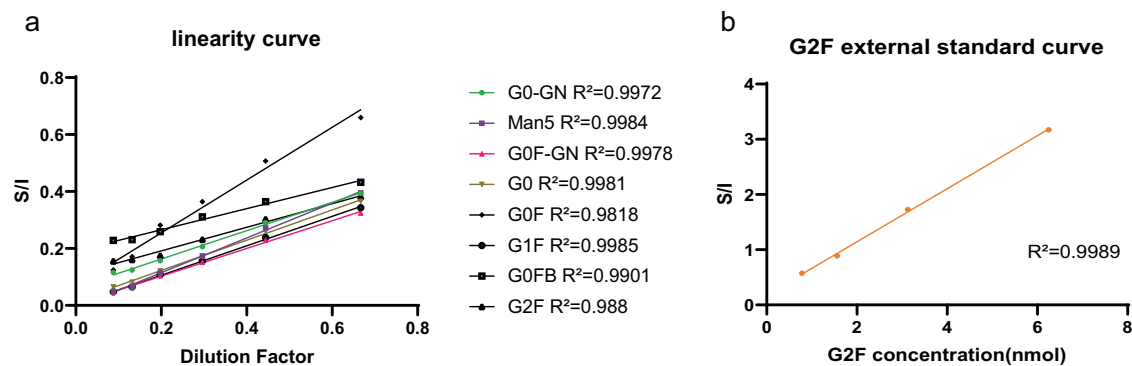


Fig. 2 | Linear range. **a** linearity of the glycans included in the method validation across a broad dilution range. Each line represents the linearity curve for a target N-glycan, with the x-axis showing the S/I (Sample to Internal standard ratio) and the y-axis representing the Dilution Factor. **b** External standard curve of G2F.

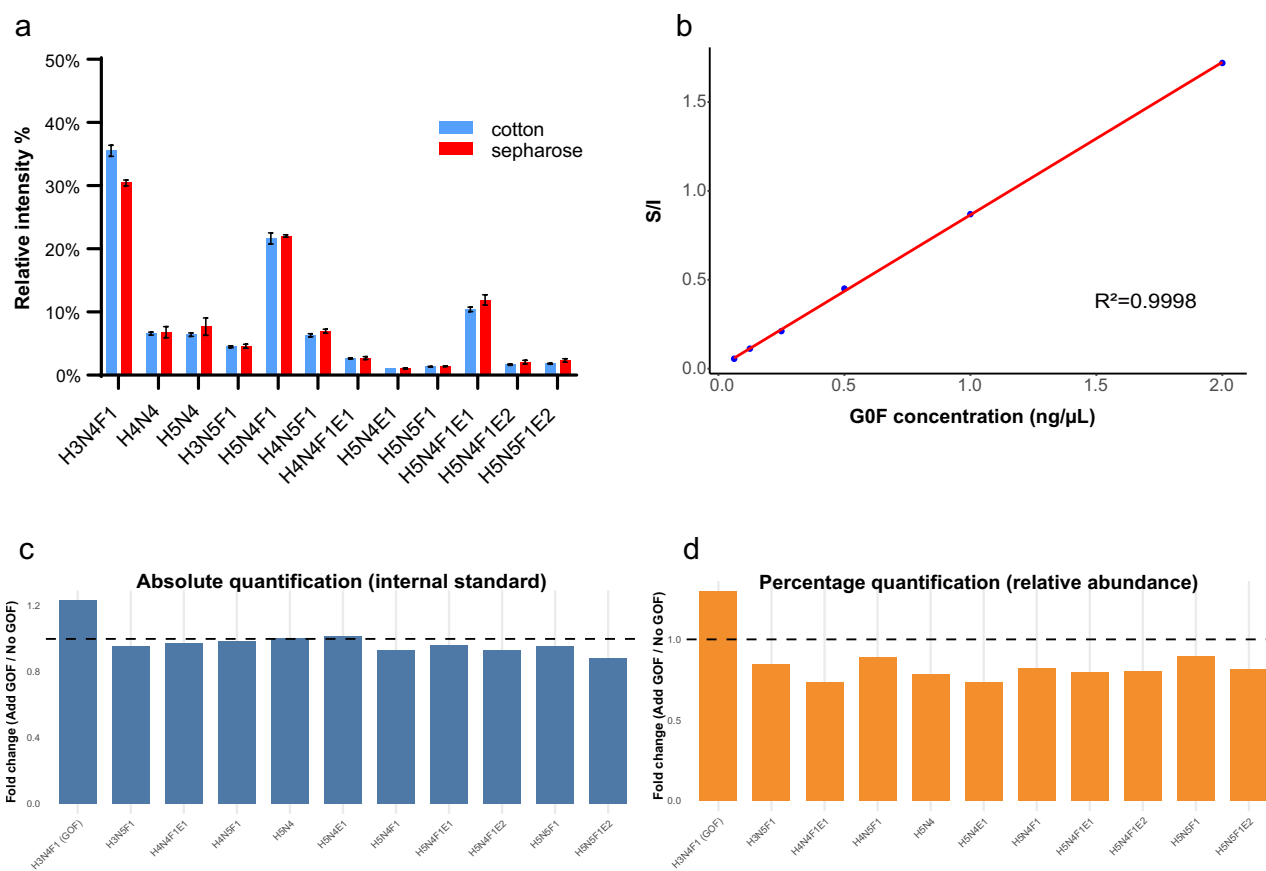


Fig. 3 | Advantages of internal-standard quantification. **a** Relative-intensity profiles of the IgG N-glycans obtained after HILIC clean-up on hand-packed cotton micro-tips (blue) and on pre-packed Sepharose CL-4B plates (red). Error bars, mean \pm SD ($n = 3$). **b** Calibration of the reduced internal standard. The signal ratio (S/I) plotted against the amount of G0F added gives a linear fit over 0.05–1.7

($R^2 = 0.9998$). **c** Fold-change in glycan abundance after spiking the sample with G0F, calculated by the internal-standard workflow. Only the spiked G0F increases (left bar); all other glycans remain essentially unchanged. **d** The same dataset processed without internal standard. Although G0F still rises, every other glycan appears to fall, illustrating the systematic bias introduced when an internal standard is not used.

variations, even in low-abundance glycans, that could impact therapeutic efficacy.

Reproducibility is crucial for any analytical method intended for large-scale production environments. Our method demonstrated excellent reproducibility in terms of sample preparation and intermediate precision across multiple experiments and biological replicates, as validated with trastuzumab samples from different monoclonal cell lines. Notably, even for low-abundance glycans, which are typically challenging owing to poor reproducibility, we achieved a coefficient of variation of approximately 10%.

This level of consistency ensures the method's ability to rapidly detect batch-to-batch variability.

We successfully established a broad quantitative linear range that meets the demands of biopharmaceutical production. This wide linear range makes our method suitable for initial screening of samples with significant differences in N-glycan levels. Additionally, this feature facilitates absolute quantitation using MALDI-MS. Using our method, we demonstrated the ability to conduct absolute quantitation, with both calibration curve establishment and sample analysis completed exceptionally quickly. This enables effective monitoring of key glycan types, offering new insights into how

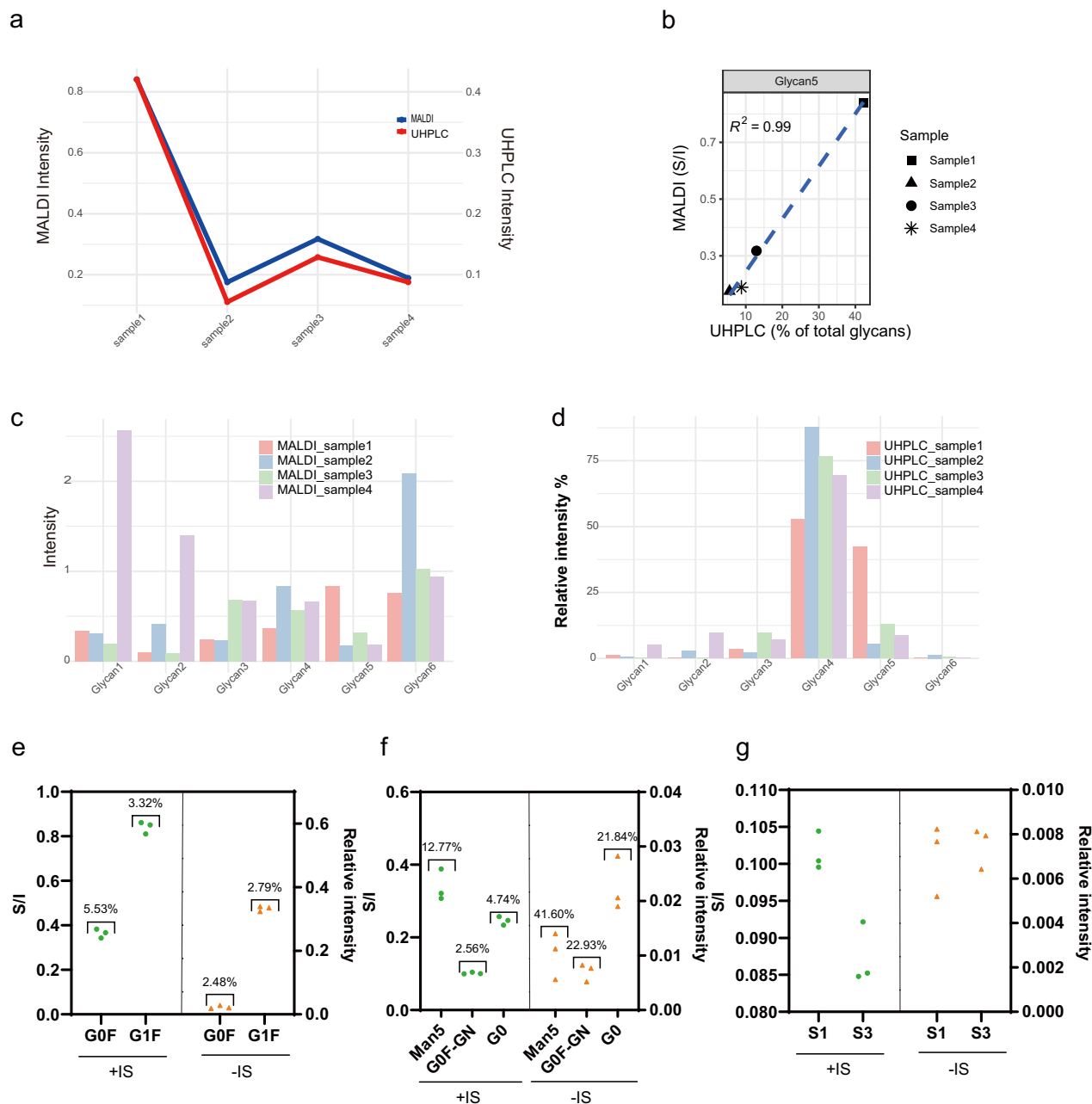


Fig. 4 | Application in cell line selection. Glycans 1–6: Man5, G0F-GN, G0, G0F, G1F and G0FB. **a** Example trend plot for Glycan 5 (G1F). MALDI intensities obtained with the +3 Da internal standard (left y-axis) parallel the UHPLC percentages (right y-axis) across all four lots. **b** Correlation between MALDI and UHPLC for the same glycan; least-squares fit gives $R^2 = 0.99$. Symbols denote individual lots. **c** Absolute MALDI read-outs (internal-standard normalisation) for Glycans 1–6 in the four lots. **d** UHPLC results (percentage values) for Glycans 1–6 in the four lots. **e** High-abundance glycans (> 10% of the total pool). Triplicate measurements of G0F and G1F acquired with (+ IS, green circles) or without (–IS, orange triangles) internal standards. Data obtained with the +IS workflow are

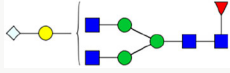
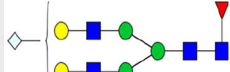
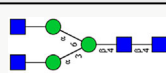
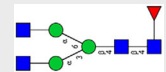
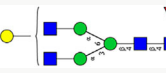
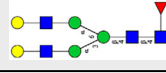
expressed as the signal-to-internal-standard ratio (S/I; left ordinate), whereas –IS data are plotted as relative intensity% (right ordinate). Braces indicate coefficients of variation (CV). **f** Low-abundance glycans (< 10%). The same comparison for Man5, G0F-GN, and G0. The +IS method retains CVs $\leq 12.8\%$, while the variability of the –IS measurements rises markedly (CV = 21.8–41.6%). **g** Impact on sample discrimination. Relative levels of a representative low-abundance glycan in two process batches (S1 and S3), each analysed in triplicate. The tighter dispersion afforded by the +IS workflow allows the between-batch difference to be resolved, whereas the greater scatter in the –IS data obscures this distinction.

changes in absolute glycan levels affect biological functionality. Such monitoring can improve our understanding of the relationship between glycosylation and drug efficacy, providing valuable insights for the development of more effective therapeutics.

To validate the method in an actual production setting, we randomly selected four trastuzumab samples from different monoclonal cell lines and demonstrated that our approach effectively identified variations in glycan

profiles. The results confirmed the method's practicality for rapidly detecting variability in large-scale antibody production, allowing us to identify the most suitable clones before applying more labor-intensive quality control methods, such as UHPLC²⁷, thereby significantly reducing the overall workload. Combined with its high-throughput analysis capability, this method is particularly well suited for rapid decision-making during cell line selection. By employing this approach during glycan

Table 2 | Stability Verification of Sialic Acid and Other N-Glycans

Glycan	Putative Structure	Composition	Sample MW(M + Na)	CV
G1F + SA		H4N4F1L1	1920.69	9.07%
G2F + SA		H5N4F1L1	2082.75	13.22%
G0		H3N4	1339.50	9.92%
G0F		H3N4F1	1282.48	13.63%
G1F		H4N4F1	1647.61	12.27%
G2F		H5N4F1	1809.66	10.92%

screening, significant time and resources can be saved, especially in the early development stages when hundreds of clones are evaluated.

Our MALDI-MS-based method has several potential applications: (1) Initial large-scale screening: This method is well suited for rapid analysis of large sample volumes, making it ideal for early-stage clone selection. (2) Process optimization: The ability to quickly detect glycan variability can guide adjustments in production processes, ensuring consistency and quality^{28,29}. (3) Absolute glycan quantitation to guide cell line engineering: By enabling accurate absolute quantitation of glycans, our method supports the modification of production cell lines to improve desired glycan characteristics³⁰. These capabilities, along with its high throughput, speed, and cost efficiency, make our method a valuable tool at various stages of biopharmaceutical development, serving as a powerful complement to traditional glycan analysis techniques.

Methods

Materials and reagents

The trastuzumab originator Herceptin® was purchased from Roche. In addition, EPO was purchased from 3SBIO, and mini-pool trastuzumab samples were generously provided by Tanshi Biotech. Sodium dodecyl sulfate (SDS), 1-hydroxybenzotriazole monohydrate (HOBt), super-2,5-dihydroxybenzoic acid (super-DHB), sodium borodeuteride (NaBD₄), and trifluoroacetic acid (TFA) were obtained from Sigma-Aldrich. The glycan standard G2F (>98%, 1787 Da) was kindly provided by professor Tiejai Li's lab (Shanghai Institute of Materia Medica, Chinese Academy of Sciences). Peptide N-glycosidase F (PNGase F) and nonylphenyl-polyethylene glycol (NP-40) were obtained from New England Biolabs. The bicinchoninic acid (BCA) protein assay kit was purchased from Thermo Fisher. Chromatography-grade acetonitrile (ACN), ethanol (EtOH), and formic acid (FA) were acquired from Merck, whereas ethyl(dimethylaminopropyl) carbodiimide (EDC) was sourced from Fluorochem.

N-Glycan release and purification for therapeutic antibodies

The therapeutic antibody was purified via Protein G Bestarose 4FF agarose beads (Bestchrom). N-glycans were released from purified IgG via PNGase F and purified via Sepharose™ CL-4B (Sigma-Aldrich). For each sample, 30 µg of IgG was quantified and dissolved in 5 µL of water. Two volumes of 2% SDS were added, and the mixture was incubated at 60 °C in a

Table 3 | Stability Verification of EPO N-Glycans

No	Composition	Sample MW(M + Na)	CV
A1	H6N2P1	1521.424	5.43%
A2	H5N4F1S2	2355.809	2.05%
A3	H6N5F1S2	2720.941	9.03%
A4	H6N5F1S3	2994.026	8.51%
A5	H7N6F1S2	3086.073	7.86%
A6	H7N6F1S3	3359.158	12.13%
A7	H7N6F1S4	3632.243	12.75%
A8	H8N7F1S3	3724.29	9.86%

thermomixer for 10 minutes. After cooling to room temperature, 10 µL of digestion buffer (4% NP-40 in a 1:1 ratio of 5x PBS) and 1 µL of PNGase F (diluted 10-fold with water) were added to the denatured IgG solution. The mixture was then incubated at 37 °C for 1 h. The sialic acid on the released glycans was protected through derivatization. Freshly prepared derivatization reagent (250 mM EDC and 250 mM HOBt in ethanol) was used for derivatization, and the mixture was incubated at 37 °C for 1 h. Prior to purification, an equal volume of acetonitrile was added to the derivatized released oligosaccharides, and the sample was prepared for purification on the basis of a previously reported protocol³¹. Following the activation and equilibration of Sepharose™ CL-4B per the manufacturer's instructions, the N-glycan-released IgG samples were applied, incubated at room temperature, and washed to remove impurities. The purified N-glycans were then eluted with water.

N-Glycan release and purification for EPO

Modifications were made to previously published methods²⁵. Specifically, denaturation was achieved by incubating EPO in 100 mM FA at room temperature for 15 minutes, followed by drying at 60 °C. The dried sample was reconstituted in 10 µL of PBS containing 1% NP-40 and 0.5 U of PNGase F and incubated at 37 °C for 1 h to release the glycans. The sialic acids were derivatized as described above and then captured using internally prepared hydrophilic interaction liquid chromatography-solid phase extraction (HILIC-SPE) pipette tips. Finally, the glycans were eluted in 10 µL of water.

Internal standard preparation

For internal standard preparation, the post-digestion product containing 30 µg of IgG was dried using a centrifugal vacuum concentrator and reconstituted with water. During this process, we optimized the protein handling procedure by reducing the cumbersome protein precipitation steps and further minimizing the amount of protein required. Ethanol was then added to a final volume of 50 µL. The mixture was incubated with 1% formic acid at 37 °C for 2 h. Subsequently, 20 µL of 2 M NaBD₄ solution was added, and the mixture was incubated at 60 °C for another 2 h. Finally, the N-glycans were purified using Sepharose™ CL-4B, an innovation that enables high-throughput internal standard preparation and aligns seamlessly with the high-throughput workflow. The purified N-glycans were then dried via centrifugation and reconstituted in 10 µL of water to serve as the internal standard. The preparation of the EPO N-glycan internal standard followed a similar procedure using 30 µg of EPO, with adjustments specific to the protein. This process involves a single-step glycan reduction reaction, resulting in a consistent 3 Da mass difference in the relative masses of all N-glycans. The method demonstrates exceptionally high reducing efficiency, ensuring accurate and unaffected quantification (Supplementary Fig. 7).

MALDI-TOF-MS analysis

For MALDI-MS analysis, a TOFMix peptide calibration standard (LaserBio Laboratories) was used to calibrate the mass spectrometer. A 1 µL aliquot of

the sample mixture containing released glycans and the corresponding internal standard was spotted onto a standard MALDI target plate (Bruker) and allowed to air dry. Subsequently, 1 μ L of super 2,5-DHB solution was spotted onto the dried sample and allowed to air dry. Each sample was spotted in triplicate. The analysis was performed using a Bruker ultrafleXtreme MALDI-TOF-MS equipped with a Smartbeam-II laser in positive ion reflector mode to detect dried N-glycans on an MTP 384 target plate. The relevant mass spectrometry parameters were: m/z range of 1000–4600; laser emission set at 10 k with a frequency of 2000 Hz; and random walk mode with 10 shots per raster spot. The laser voltage was set at 80 V.

Data processing

Raw MALDI-TOF spectra were processed in Bruker flexAnalysis v 3.4. Peak lists were generated with the Mass List Find function (SUM algorithm) and filtered for a signal-to-noise ratio ≥ 3 . Glycan assignments were made in GlycoWorkbench and the corresponding peaks were batch-extracted in BioPharma 3. Quantification used a single isotope peak: the first isotopic $[M]^+$ intensity for glycans below m/z 2000 and the second satellite $[M + 1]^+$ intensity for larger glycans. The relative quantity of each N-glycan was calculated on the basis of the ratio of signal intensity (sample to internal standard, S/I).

Data availability

The glycan-related source data are provided in the Supplementary Data. All mass spectrometry data used in this work are available from the authors upon request.

Received: 21 February 2025; Accepted: 29 August 2025;

Published online: 02 October 2025

References

- Rocamora, F. et al. Glycosylation shapes the efficacy and safety of diverse protein, gene and cell therapies. *Biotechnol. Adv.* **67**, 108206 (2023).
- Delobel, A. Glycosylation of Therapeutic Proteins: A Critical Quality Attribute. *Methods Mol. Biol.* **2271**, 1–21 (2021).
- Moremen, K. W., Tiemeyer, M. & Nairn, A. V. Vertebrate protein glycosylation: diversity, synthesis and function. *Nat. Rev. Mol. Cell Biol.* **13**, 448–462 (2012).
- Zhang, L., Luo, S. & Zhang, B. Glycan analysis of therapeutic glycoproteins. *MAbs* **8**, 205–215 (2016).
- Shrivastava, A., Joshi, S., Guttman, A. & Rathore, A. S. N-Glycosylation of monoclonal antibody therapeutics: A comprehensive review on significance and characterization. *Anal. Chim. Acta* **1209**, 339828 (2022).
- Vattepu, R., Sneed, S. L. & Anthony, R. M. Sialylation as an Important Regulator of Antibody Function. *Front Immunol.* **13**, 818736 (2022).
- Kaur, H. Characterization of glycosylation in monoclonal antibodies and its importance in therapeutic antibody development. *Crit. Rev. Biotechnol.* **41**, 300–315 (2021).
- Sha, S., Agarabi, C., Brorson, K., Lee, D. Y. & Yoon, S. N-Glycosylation Design and Control of Therapeutic Monoclonal Antibodies. *Trends Biotechnol.* **34**, 835–846 (2016).
- Hua, S. et al. Technologies for glycomic characterization of biopharmaceutical erythropoietins. *TrAC Trends Anal. Chem.* **68**, 18–27 (2015).
- Thomson, R. I. et al. Analysis of three epoetin alpha products by LC and LC-MS indicates differences in glycosylation critical quality attributes, including sialic acid content. *Anal. Chem.* **89**, 6455–6462 (2017).
- Sokolov, M. et al. Robust factor selection in early cell culture process development for the production of a biosimilar monoclonal antibody. *Biotechnol. Prog.* **33**, 181–191 (2017).
- Walsh, G. Biopharmaceutical benchmarks 2018. *Nat. Biotechnol.* **36**, 1136–1145 (2018).
- Sandra, K., Steenbeke, M., Vandenheede, I., Vanhoenacker, G. & Sandra, P. The versatility of heart-cutting and comprehensive two-dimensional liquid chromatography in monoclonal antibody clone selection. *J. Chromatogr. A* **1523**, 283–292 (2017).
- Traylor, M. J. et al. Comprehensive Discovery and Quantitation of Protein Heterogeneity via LC-MS/MS Peptide Mapping for Clone Selection of a Therapeutic Protein. *Anal. Chem.* **88**, 9309–9317 (2016).
- Costa, A. R., Rodrigues, M. E., Henriques, M., Oliveira, R. & Azeredo, J. Glycosylation: impact, control and improvement during therapeutic protein production. *Crit. Rev. Biotechnol.* **34**, 281–299 (2014).
- Fan, Y. et al. Amino acid and glucose metabolism in fed-batch CHO cell culture affects antibody production and glycosylation. *Biotechnol. Bioeng.* **112**, 521–535 (2015).
- Wang, Q., Chung, C. Y., Chough, S. & Betenbaugh, M. J. Antibody glycoengineering strategies in mammalian cells. *Biotechnol. Bioeng.* **115**, 1378–1393 (2018).
- Hajba, L., Szekrényes, Á, Borza, B. & Guttman, A. On the glycosylation aspects of biosimilarity. *Drug Discov. Today* **23**, 616–625 (2018).
- Qin, W. et al. Providing Bionic Glycome as internal standards by glycan reducing and isotope labeling for reliable and simple quantitation of N-glycome based on MALDI-MS. *Anal. Chim. Acta* **1081**, 112–119 (2019).
- Reiding, K. R., Blank, D., Kuijper, D. M., Deelder, A. M. & Wuhrer, M. High-throughput profiling of protein N-glycosylation by MALDI-TOF-MS employing linkage-specific sialic acid esterification. *Anal. Chem.* **86**, 5784–5793 (2014).
- Kim, S. et al. Drifts in ADCC-related quality attributes of Herceptin®: Impact on development of a trastuzumab biosimilar. *MAbs* **9**, 704–714 (2017).
- Uversky, V. N. & Redwan, E. M. Erythropoietin and co.: intrinsic structure and functional disorder. *Mol. Biosyst.* **13**, 56–72 (2016).
- Jurado García, J. M., Torres Sánchez, E., Olmos Hidalgo, D. & Alba Conejo, E. Erythropoietin pharmacology. *Clin. Transl. Oncol.* **9**, 715–722 (2007).
- Lippold, S., Thavarajah, R., Reusch, D., Wuhrer, M. & Nicolardi, S. Glycoform analysis of intact erythropoietin by MALDI FT-ICR mass spectrometry. *Anal. Chim. Acta* **1185**, 339084 (2021).
- Falck, D. et al. Affinity purification of erythropoietin from cell culture supernatant combined with MALDI-TOF-MS analysis of erythropoietin N-glycosylation. *Sci. Rep.* **7**, 5324 (2017).
- Huffman, J. E. et al. Comparative performance of four methods for high-throughput glycosylation analysis of immunoglobulin G in genetic and epidemiological research. *Mol. Cell. Proteom.* **13**, 1598–1610 (2014).
- Trbojević-Akmačić, I., Vilaj, M. & Lauc, G. High-throughput analysis of immunoglobulin G glycosylation. *Expert Rev. Proteom.* **13**, 523–534 (2016).
- Patel, T. P., Parekh, R., Moellering, B. & Prior, C. Different culture methods lead to differences in glycosylation of a murine IgG monoclonal antibody. *Biochemical J.* **285**, 839–845 (1992).
- Mack, G. FDA balks at Myozyme scale-up. *Nat. Biotechnol.* **26**, 592 (2008).
- Reddy, J. V., Raudenbush, K., Papoutsakis, E. T. & Ierapetritou, M. Cell-culture process optimization via model-based predictions of metabolism and protein glycosylation. *Biotechnol. Adv.* **67**, 108179 (2023).
- Reiding, K. R., Lonardi, E., Hipgrave Ederveen, A. L. & Wuhrer, M. Ethyl Esterification for MALDI-MS Analysis of Protein Glycosylation. *Methods Mol. Biol.* **1394**, 151–162 (2016).

Acknowledgements

The authors acknowledge that Fig. 1 was created with BioRender.com. This work was supported by the grant from the National Key R&D Program of China (2022YFC3400800) and the National Natural Science Foundation of China (32071276).

Author contributions

S.-F.R. developed the research idea; W.-L.Z., S.-F.R. designed the research; W.-L.Z. performed the experiments and analyzed the data; H.-J.Z. L.-Q.X. and X.-N.M. provided essential experimental assistance; W.-L.Z. and S.-F.R. wrote the paper, which was critically read and approved by all others.

Competing interests

The authors declare no competing interests.

Additional information

Supplementary information The online version contains supplementary material available at

<https://doi.org/10.1038/s42004-025-01680-2>.

Correspondence and requests for materials should be addressed to Shifang Ren.

Peer review information *Communications Chemistry* thanks the anonymous reviewers for their contribution to the peer review of this work.

Reprints and permissions information is available at <http://www.nature.com/reprints>

Publisher's note Springer Nature remains neutral with regard to jurisdictional claims in published maps and institutional affiliations.

Open Access This article is licensed under a Creative Commons Attribution-NonCommercial-NoDerivatives 4.0 International License, which permits any non-commercial use, sharing, distribution and reproduction in any medium or format, as long as you give appropriate credit to the original author(s) and the source, provide a link to the Creative Commons licence, and indicate if you modified the licensed material. You do not have permission under this licence to share adapted material derived from this article or parts of it. The images or other third party material in this article are included in the article's Creative Commons licence, unless indicated otherwise in a credit line to the material. If material is not included in the article's Creative Commons licence and your intended use is not permitted by statutory regulation or exceeds the permitted use, you will need to obtain permission directly from the copyright holder. To view a copy of this licence, visit <http://creativecommons.org/licenses/by-nc-nd/4.0/>.

© The Author(s) 2025